

Article

Preparation and Characterization of a LiFePO_4 - Lithium Salt Composite Cathode for All-Solid-State Li-Metal Batteries

Debabrata Mohanty ¹, Pin-Hsuan Huang ¹ and I-Ming Hung ^{1,2,*}

¹ Department of Chemical Engineering and Materials Science, Yuan Ze University, 135 Yuan-Tung Road, Chung-Li 32003, Taiwan

² Hierarchical Green-Energy Materials (Hi-GEM) Research Center, National Cheng Kung University, Tainan 70101, Taiwan

* Correspondence: imhung@saturn.yzu.edu.tw; Tel.: +886-3-463-8800

Abstract: This study develops a composite cathode material suitable for solid-state Li-ion batteries (SSLIB). The composite cathode consists of LiFePO_4 as the active material, Super P and KS-4 carbon materials as the conductive agents, and LiTFSI as the lithium salt. An LiFePO_4 /LATP-PVDF-HFP/Li all-solid-state LIB was assembled using $\text{Li}_{1.3}\text{Al}_{0.3}\text{Ti}_{1.7}(\text{PO}_4)_3$ (LATP)/ poly(vinylidene fluoride-co-hexafluoropropylene (PVDF-HFP) as the solid-state electrolyte and lithium metal as the anode. The structure of the synthesized LATP was analyzed using X-ray diffraction, and the microstructure of the composite cathode and solid electrolyte layer was observed using a field emission scanning electron microscope. The electrochemical properties of the all-solid-state LIB were analyzed using electrochemical impedance spectroscopy (EIS) and a charge–discharge test. The effect of the composition ratio of the fabricated cathode on SSLIB performance is discussed. The results reveal that the SSLIB fabricated using the cathode containing LiFePO_4 , Super P, KS-4, PVDF, and LiTFSI at a weight ratio of 70:10:10:7:3 (wt.%) and a LATP/PVDF-HFP solid electrolyte layer containing PVDF-HFP, LiTFSI, and LATP at a weight ratio of 22:33:45 (wt.%) exhibited the optimal performance. Particularly, the SSLIB fabricated using the cathode containing 3% LiTFSI exhibited a discharge capacity of 168.9 mAhg^{-1} at 0.1 C, which is close to the theoretical capacity (170 mAhg^{-1}), and had very good stability. The findings of this study suggests that the incorporation of an appropriate amount of LiTFSI can significantly enhance the electrochemical performance of SSLIB batteries.

Keywords: composite cathode; LiFePO_4 ; LATP; electrochemical performance



Citation: Mohanty, D.; Huang, P.-H.; Hung, I.-M. Preparation and Characterization of a LiFePO_4 -Lithium Salt Composite Cathode for All-Solid-State Li-Metal Batteries. *Batteries* **2023**, *9*, 236. <https://doi.org/10.3390/batteries9040236>

Academic Editor: Yong-Joon Park

Received: 23 February 2023

Revised: 14 April 2023

Accepted: 19 April 2023

Published: 20 April 2023



Copyright: © 2023 by the authors. Licensee MDPI, Basel, Switzerland. This article is an open access article distributed under the terms and conditions of the Creative Commons Attribution (CC BY) license (<https://creativecommons.org/licenses/by/4.0/>).

1. Introduction

Lithium-ion batteries (LIBs) have attracted significant attention as an energy storage technology owing to their high energy density, long cycle life, and low self-discharge rate [1]. However, LIBs present safety issues caused by the unstable and combustible liquid alkyl-carbonate-based electrolytes frequently used in commercial LIBs [2,3]. These issues are particularly crucial in the development of various devices and electric vehicles that require significant energy storage [4].

All-solid-state lithium metal polymer batteries with flexible thin films as the anode, electrolyte, and cathode enable flexible battery assembly and a broad range of battery shape/design adaptations as well as enhanced safety and efficiency [5]. Lithium metal polymer batteries exhibit high cell potentials and energy densities owing to the low atomic weight and strong electropositive potential of lithium metal; however, the cathode active material used in these batteries has restricted their further application [6]. Among the various cathode materials used in lithium metal batteries, lithium iron phosphate (LiFePO_4) has attracted significant attention owing to its high theoretical capacity (170 mAhg^{-1}), good thermal stability, and long-term cycling performance [7–9]. As is known for carbon-coated particles and for conducting polymer coatings, which may also be used to protect

the aluminum current collector from oxidation, LiFePO₄-based positive electrodes, with enhanced electric conductivity between the electrode's interphases when LiTFSI-based electrolytes are utilized, allow particularly high -rate capability [10–12]. Additionally, compared to lithium, LiFePO₄ exhibits a reversible electrode potential of approximately 3.5 V, making it suitable for usage with hybrid electrolytes [13,14]. Furthermore, LiFePO₄ has been reported to contain abundant elemental iron, which is good for the environment [15]. Several studies have investigated the potential of LiFePO₄ as a positive electrode [16,17]. However, its poor electronic conductivity and low -rate capability have limited its practical application [18,19]. To overcome these limitations, various approaches have been proposed, such as the use of conductive agents [20,21]. Lithium salt addition is a promising strategy to enhance the rate capability and ionic conductivity of electrodes for solid-state LIBs. For example, lithium bis(trifluoromethanesulfonyl)imide (LiTFSI), a commonly used lithium salt, has been demonstrated to improve the electrochemical performance of LiFePO₄-based LIBs [22,23] and to improve mechanical stability and interfacial contact between the cathode and electrolyte [24,25].

Another important aspect of solid-state lithium-ion batteries (SSLIBs) is the use of solid electrolytes [26,27]. Solid-state electrolytes exhibit higher thermal stability and mechanical strength than liquid electrolytes, thus reducing the risk of leakage and thermal runaway, and improving the safety of batteries [28–30]. Poly(vinylidene fluoride-co-hexafluoropropylene) (PVDF-HFP) is a widely used solid electrolyte for SSLIBs owing to its high ionic conductivity and excellent mechanical properties [31,32].

In this study, we aimed to develop a composite cathode material suitable for SSLIBs by mixing LiFePO₄, Super P, KS-4, and LiTFSI as cathode materials. In addition, LATP was added to the PVDF-HFP, and the composite was used as the solid-state electrolyte layer. At ambient temperature, LATP exhibits air- and water-resistant properties, as well as a high lithium-ion conductivity of up to $5 \times 10^{-4} \text{ S cm}^{-1}$ [33,34]. The addition of a hexafluoropropylene (HFP) group to PVDF-HFP suppressed the crystallinity of PEO suppressed, thereby enhancing its ionic conductivity [35]. In addition, LATP was added to the PVDF-HFP, and the LATP/PVDF-HFP electrolyte exhibited a low capacity during the rapid charge/discharge test owing to the high interface impedance between it and the positive electrode [36]. The pores formed in the cathode hinder the rapid passage of lithium-ions into the electrolyte layer, resulting in a high resistance and a low battery capacity, particularly at a high charging and discharging rate [37]. To increase the lithium-ion conductivity of the cathodes, in this study, lithium salt was added to the cathode, and the effect of the ratio of lithium salt to binder in the cathode was investigated. The findings of this study will shed light on the optimization of LiFePO₄-based LIBs via the addition of lithium salt, and contribute to the pioneering of high-performance SSLIBs for practical purposes.

2. Results and Discussion

Figure 1 shows the structure and properties of the LATP ceramic powder prepared using the sol-gel method, and the image reveals that the structure and properties are consistent with the standard product. X-ray diffraction (XRD) results, which were utilized to investigate the crystalline structure of LATP powder, revealed that the diffraction peaks of the LATP powder were consistent with the standard diffraction pattern of JCPDS 35-0754 (Figure 1a). The mole ratio Li:Al:Ti:P was 1.25:0.32:1.79:3.13, which was determined by ICP-AES. Figure 1b shows the diffraction peaks of the LATP/PVDF-HFP composite electrolyte membrane containing LATP powder, PVDF-HFP, and LiTFSI at a ratio of 45:22:33 (wt.%). The positions of the main crystallization peaks of pure PVDF-HFP can be observed in the XRD pattern in Figure 1c. After the PVDF-HFP polymer was mixed with LATP, the crystallization peaks of LATP appeared in the XRD pattern, indicating the successful incorporation of LATP into the electrolyte membrane. The XRD pattern of the LATP/PVDF-HFP composite electrolyte membrane revealed that the addition of LATP nanoparticles into the polymer resulted in a decrease in the signal of the PVDF-HFP crystallization peak,

indicating that the addition of LATP decreased the crystallinity of PVDF-HFP, thus enhancing the ionic conductivity of the LATP/PVDF-HFP composite electrolyte [38]. LATP is a high-crystallinity ceramic particle; thus, it can be used as a nucleating agent to induce the formation of smaller and less ordered crystals in the PVDF-HFP matrix. Consequently, this results in a reduction in the overall crystallinity of the composite material [39]. The addition of LATP resulted in a decrease in the crystallinity of the PVDF-HFP polymer, thereby improving its ion conductivity.

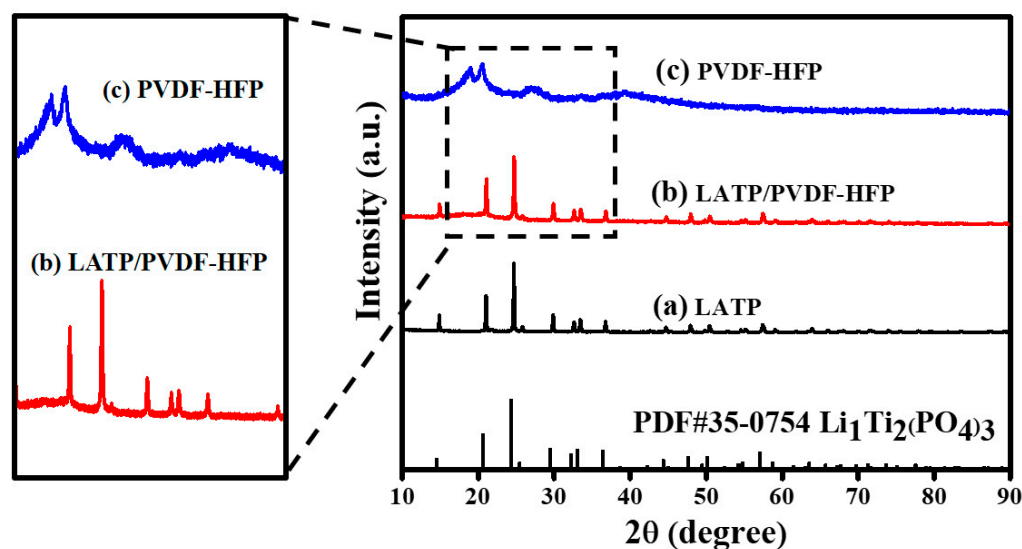


Figure 1. X-ray diffraction (XRD) patterns of (a) $\text{Li}_{1.3}\text{Al}_{0.3}\text{Ti}_{1.7}(\text{PO}_4)_3$ powder, (b) LATP/PVDF-HFP composite electrolyte membrane, and (c) pure PVDF-HFP.

LATP nano-ceramic materials are incredibly small, which enable their agglomeration, thus preventing the ability of PVDF-HFP polymers to effectively fill the gaps between the ceramic materials. Consequently, these gaps formed holes and increased the interface impedance. In addition, the pores formed by the agglomeration phenomenon hinders the transport and mobility of lithium ions, and increase the interface impedance between the formed LATP/PVDF-HFP electrolyte membrane and the positive electrode material. To prevent the agglomeration of the LATP in the PVDF-HFP electrolyte membrane, the LATP/PVDF-HFP composite was subjected to planetary ball milling to achieve simultaneous revolution and rotation during mixing when preparing the electrolyte slurry. The distribution of nano-sized LATP powders in the PVDF-HFP polymer was observed using field emission scanning electron microscopy (FE-SEM; Figure 2). The image revealed that the composite electrolyte membrane containing 45% LATP exhibited the most compact structure (Figure 2b). In contrast, the composite electrolyte membrane containing 40% LATP contained notable holes (Figure 2a). In addition, some holes were observed in the composite electrolyte membrane containing 55% LATP (Figure 2c). The positive electrode material and LATP/PVDF-HFP electrolyte were fabricated using the procedure described in the materials and methods section of this article. The positive electrode/LATP/PVDF-HFP interface was investigated using FE-SEM, as shown in Figure 3. The FE-SEM image reveals the uniform interface of the positive electrode sheet without LiTFSI and the positive electrode material containing LiTFSI-3% with the LATP/PVDF-HFP electrolyte membrane. However, the delamination between the positive electrode and the LATP/PVDF-HFP electrolyte was notable, resulting in high interfacial resistance.

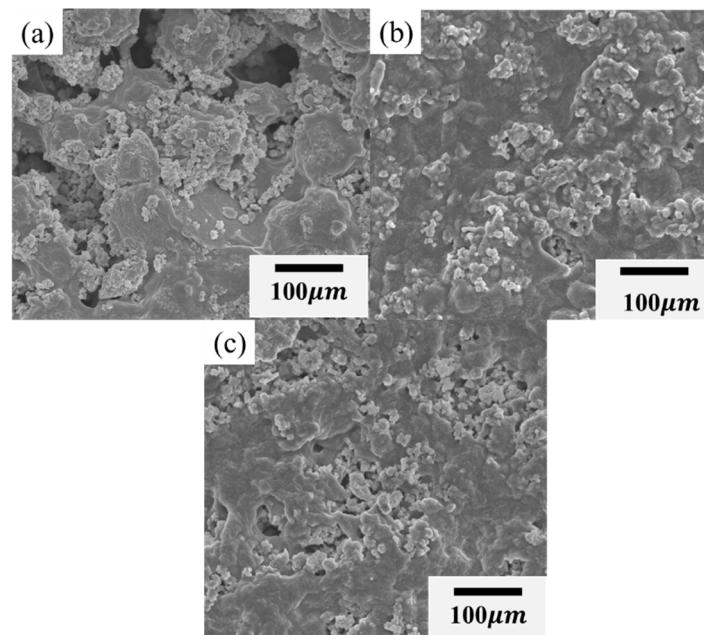


Figure 2. Field emission scanning electron microscopy (FE-SEM) images of electrolyte membranes prepared with different LATP contents: (a) LATP-40%, (b) LATP-45%, and (c) LATP-55%.

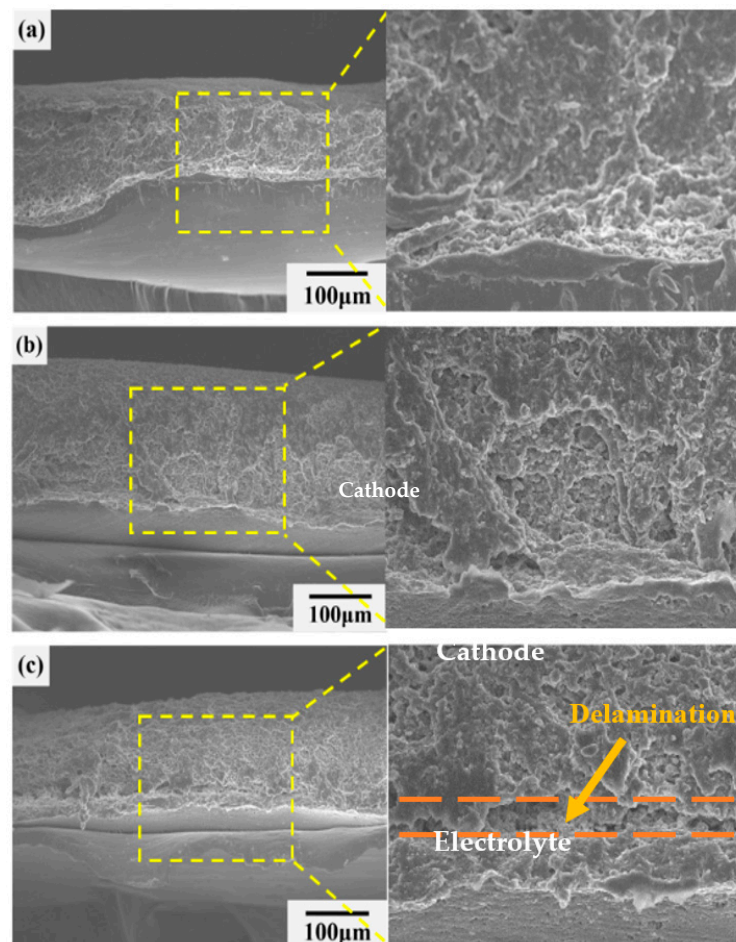


Figure 3. FE-SEM images of composite cathode sheets with different LiTFSI contents: (a) LiTFSI-0%, (b) LiTFSI-3%, and (c) LiTFSI-4% on a LATP/PVDF-HFP electrolyte membrane.

The internal impedance of the material was analyzed using AC impedance, and the impedances of the samples under different conditions were tested at room temperature. To test the resistance of the battery, a coin cell battery was used with an X% LiTFSI (X = 0, 2, 3, 4, and 5) +LiFePO₄ cathode//LATP/PVDF-HFP electrolyte membrane// Li metal assembly. Figure 4 shows the electrochemical impedance spectroscopy (EIS) results and the analogous circuit. The Nyquist plots consisted of one semicircle and one inclined line. Here, R_1 is the resistance value of the LiFePO₄ cathode material and the electrolyte and R_2 is the interface resistance allying the electrolyte and the electrodes, which includes charge transfer as well as the resistances of the electrodes. The interface impedance of the cathode with the electrolyte, C_2 , is for the electric double-layer capacitor; W_2 is the Warburg impedance of the diffusion reaction. The R_1 , R_2 , and the total resistance (R_{total}) of the LiFePO₄ and the electrolyte membrane were determined via a software using the analogous circuit.

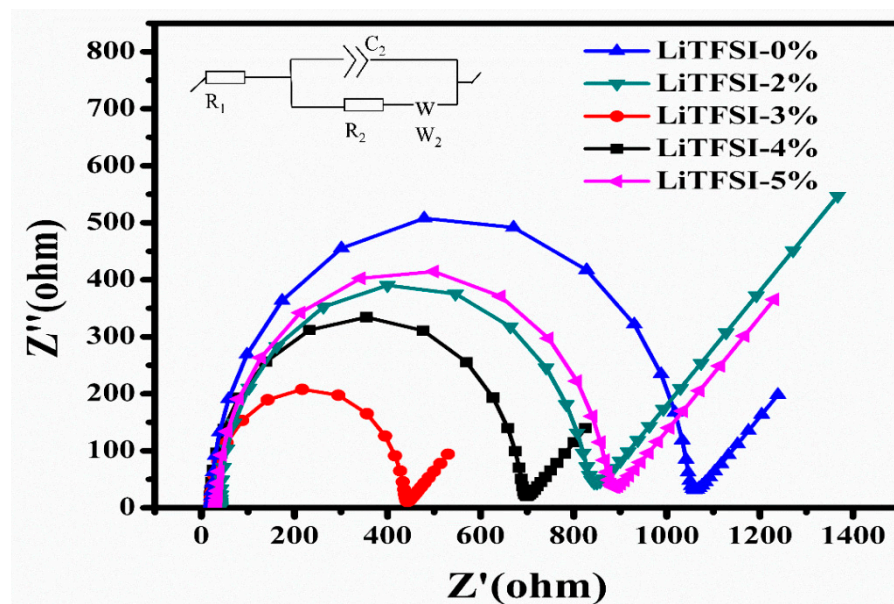


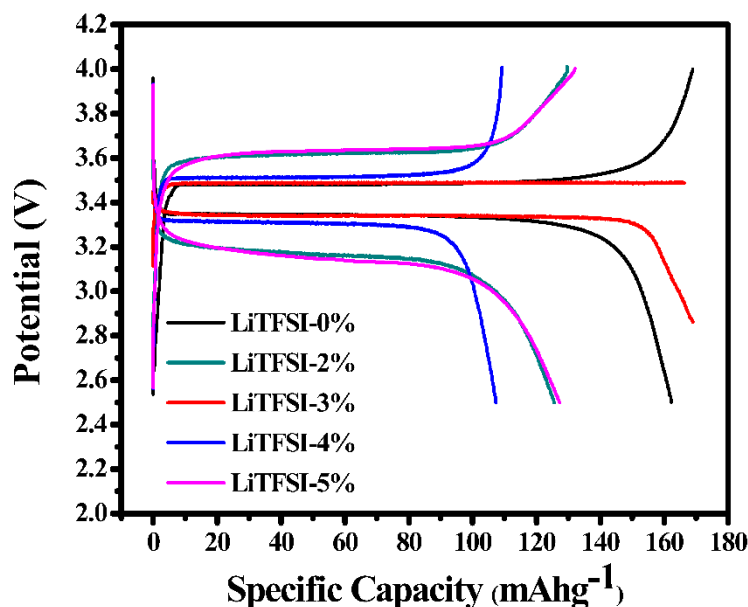
Figure 4. AC impedance spectra of the X% LiTFSI (X = 0, 2, 3, 4, and 5) +LiFePO₄ cathode//LATP/PVDF-HFP electrolyte membrane// Li cells at room temperature.

The AC impedance test results (Table 1) revealed that the total resistance values (R_{total}) of the cathodes containing LiTFSI were less than that of the sample not containing LiTFSI (LiTFSI-0%), confirming that the addition of LiTFSI effectively reduced the total resistance of the cathode. Particularly, the battery containing LiTFSI-3% exhibited the smallest resistance value, indicating a reduction in the hindrance of the internal lithium-ion transport path and the interface impedance. The differences between the experimentally measured impedance spectra and the predictor variables in the full spectral regions of all the samples were less than 10%. The resistance of the electrolyte and the component of the contact resistance are represented by the higher-frequency interception of the semicircle with the real axis of impedance. The resistance, a crucial kinetics characteristic of the cell processes, indicates the charge-transfer mechanism of the Faradic reactions occurring at the electrode–electrolyte interfaces. Furthermore, the addition of LiTFSI to the positive electrode not only reduced the total resistance of the battery but also improved the transport of lithium-ions and reduced the resistance of the interface between the electrolyte and electrodes [40]. In summary, the addition of LiTFSI to the positive electrode of the battery improved the efficiency of the battery by reducing its internal resistance and improving the transport of lithium ions [41].

Table 1. Resistances and ionic conductivity of the X% LiTFSI (X = 0, 2, 3, 4, and 5) +LiFePO₄ cathode//LATP/PVDF-HFP electrolyte membrane// Li cells.

Sample	R ₁ (Ω)	R ₂ (Ω)	R _{total} (Ω)
LiTFSI-0%	21.4	1019.0	1040.4
LiTFSI-2%	40.8	819.3	860.1
LiTFSI-3%	20.2	415.7	435.9
LiTFSI-4%	18.7	666.2	685.9
LiTFSI-5%	33.9	831.6	865.5

In this study, CR2023 cells with a configuration of X% LiTFSI (X = 0, 2, 3, 4, 5) +LiFePO₄ cathode//LATP/PVDF-HFP electrolyte membrane// Li metal anode were prepared, and their performances under continuous charge/discharge cycling at a rate of 0.1–1 C in a potential window of 2.5–4.0 V at room temperature were investigated. The galvanostatic charge-discharge curves of the cells at 25 °C are shown in Figure 5. The batteries were galvanostatically charged and discharged between 2.5 and 4.0 V (vs. Li/Li⁺) at 0.1 C. In this study, the C rate was determined using the theoretical capacity of LFP, which is 170 mAh g⁻¹. The results revealed that the batteries exhibited a notable charge–discharge plateau at a voltage of approximately 3.4 V vs. Li⁺/Li, demonstrating the presence of a dual-phase Fe³⁺/Fe²⁺ redox reaction via a first-order shift between FePO₄ and LFP [42,43]. The cells coupled with LiTFSI-0%, LiTFSI-2%, LiTFSI-3%, LiTFSI-4%, and LiTFSI-5% exhibited discharge capacities of 153.1, 125.5, 168.9, 107.3, and 127.3 mAh g⁻¹ at 0.1 C, respectively. This indicates that, compared to other samples, the SSLBs containing LiTFSI-3%-based composite LiFePO₄ cathodes exhibited larger discharge capacities and improved coulombic efficiency (>94%), demonstrating good Li⁺ reversibility throughout the charge/discharge cycling process. This result indicates that the electrochemical performance of the composite LFP cathode-based cells increased considerably at an LiTFSI concentration of 3%.

**Figure 5.** Typical charge–discharge curves of Li | LATP/PVDF-HFP | X% LiTFSI (X = 0, 2, 3, 4, 5) +LiFePO₄ cells at 0.1 C.

To test the cyclic performance of the Li | LATP/PVDF-HFP | X% LiTFSI (X = 0, 2, 3, 4, 5) +LiFePO₄ batteries, they were repeatedly charged and discharged between 2.5 and 4.0 V vs. Li/Li⁺ at room temperature (Figure 6a). The discharge capacity of the battery with the Li | LATP/PVDF-HFP | X% LiTFSI (X = 0, 2, 3, 4, 5) +LiFePO₄ configuration increased significantly during the initial cycles and stabilized with an increase in the number of cycles (Figure 6a). During the cycling test, all the SSLBs exhibited outstanding coulombic

efficiency and enhanced capacity retention (with nearly no capacity receding). The steady discharge capacity of the as-fabricated SSLBs can be attributed to three factors: the absence of iron disintegration from the composite LFP cathode [44], the strength of the solid electrolyte interphase (SEI) layer, and homogeneous Li metal precipitation during long-term cycling [45]. Compared to other composite cathodes, SSLBs fabricated using LiTFSI-3% composite cathodes exhibited greater capacity retention. Furthermore, the hybrid solid state electrolytes and the composite cathode collectively enabled the formation of a stable SEI layer structure and the homogeneous precipitation of Li metal, which increased the lifecycle of the SSLBs by reducing the production of Li dendrites. These results indicate that a Li salt-based composite cathode can be successfully used in high-voltage lithium-ion batteries (with a potential range of 2.5–4.0 V). The findings of this study will be beneficial for fabricating very stable battery materials for high-performance lithium-ion batteries that comprise composite structures made of polymers and particles. To expand on the ideal formula for enhanced cycle stability, inner resistance, electrode polarization, and rate capability, further research is required. Figure 6b shows the discharge capacity of the battery as a function of LiTFSI concentration at various C rates. The SSLBs fabricated using LiTFSI-3%-based composite cathodes exhibited a capacity retention as high as 94% during the charge/discharge cycling test at 0.1–0.5C. This further confirmed the importance of LiTFSI content for the electrochemical properties of Li | LATP/PVDF-HFP | X% LiTFSI (X = 0, 2, 3, 4, 5) + LiFePO₄ batteries in order to achieve improved specific capacity and rate capability. The addition of LiTFSI at 2, 4, and 5 wt.% led to a decrease in internal resistance but a lower capacity and rate capability compared to the bare sample. The decrease in capacity and rate capability can be attributed to the increased ionic conductivity of the electrolyte at higher concentrations of LiTFSI, which can lead to a decrease in concentration polarization and improve the internal resistance of the electrode [46]. However, at higher concentrations of LiTFSI, the electrolyte becomes more viscous, and the diffusion of lithium ions is hindered, resulting in a lower capacity and rate capability [47].

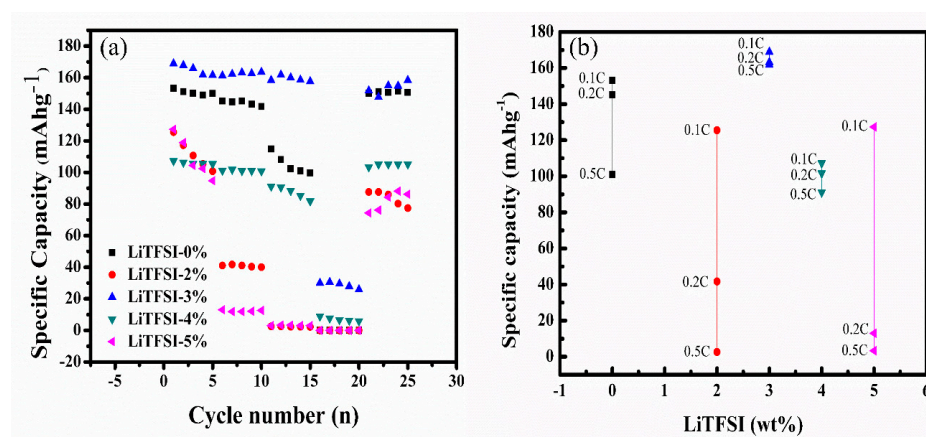


Figure 6. (a) Cyclic performance curves of Li | LATP/PVDF-HFP | X% LiTFSI (X = 0, 2, 3, 4, 5) + LiFePO₄ cells at ambient temperature and (b) the change in the discharge capacity with a change in the LiTFSI content at different C rates.

3. Materials and Methods

First, LATP nano ceramic powder was prepared using the modified sol-gel method described in our previous study [48]. Subsequently, the mixture was dried and sieved. Thereafter, LiTFSI: PVDF-HFP with a mass ratio of 3:2 and LATP powder (45% weight ratio) were added to 1-methyl-2-pyrrolidone (NMP, showa, purity: 95%) solvent. Subsequently, the mixture was stirred using a planetary ball mill at 700 rpm for 90 min to prepare the electrolyte slurry. The solution was sealed with a sealing mold to prevent solvent evaporation, after which it was heated and stirred in a heater for an entire day for the thorough dissolution of PVDF-HFP (Sigma, molecular weight: 400,000) and LiTFSI (Alfa, purity: 98%).

N-methyl pyrrolidone (NMP, showa, purity: 95%) solvent and polyvinylidene flouride (PVDF, Jingming Chemical, 99%) binders were combined and centrifuged for 1 h to remove foam. Thereafter, LiFePO_4 powder (Jingming Chemical, 98%), Super P (Taiwan Libo, 99%), and KS-4 (Taiwan Libo, 99%) were added to the mixture in a 7:1:1 ratio, and agitated using a centrifugal defoamer for 1 h. Subsequently, the mixture was uniformly distributed on the first layer of an aluminum foil using a spatula machine with a squeegee size of 100 m. Thereafter, the solution was dried in a vacuum oven at 100 °C for 8 h to eliminate the solvent. The thickness was measured using a thickness gauge after vacuuming and the complete removal of the solvent. LiTFSI-X% (X = 0, 2, 3, 4, 5, and 6) (Alfa, 98%) and NMP solvent were pre-mixed; a portion of the PVDF binder was replaced with LiTFSI lithium salt, and centrifuged for 1 h to remove foam. Thereafter, LiFePO_4 powder, Super P, and KS-4 were added to the solution at a ratio of 7:1:1, and the mixture was stirred for 1 h using a centrifugal defoamer to achieve a ratio of 70:10:10:(10-X):X for LiFePO_4 ; Super P; KS-4; PVDF; and LiTFSI. The solution was uniformly distributed on the first layer of aluminum foil using a spatula machine with a squeegee size of 100 m. Thereafter, the solution was dried in a vacuum oven at 100 °C for 8 h to eliminate the solvent. The thickness was measured using a thickness gauge after vacuum treatment and the complete removal of the solvent.

The prepared hybrid electrolyte slurry was spread uniformly on the composite cathode sheet using a tape-casting machine with a scraper size of 1000 mm. The thickness of the solid electrolyte layer was measured using a thickness gauge after the assembly was dried in a vacuum oven at 50 °C for three days. A pole piece with a 13 mm diameter circle was cut out. Thereafter, a coin cell battery was assembled by placing the pole pieces in a glove box, and adding a lithium metal negative electrode (diameter: 13 mm) and other battery components. The button battery components were stacked and assembled using a hydraulic press. The assembled coin cells were left in a glove box for a day, after which their electrochemical properties were investigated.

The pure phase of the synthesized LATP was examined using XRD (D2 phaser, Bruker). The elemental composition of LATP was determined by ICP-AES (Agilent 7500ce). The microstructure of the composite cathode and solid electrolyte layer was examined using FE-SEM (JSM 6701F, JEOL). The electrochemical properties of the SSLBs were examined using EIS (VSP-300, BioLogic) and charge–discharge testing (BAT-750B, Acu Tech), and the effect of the composition ratio of the composite cathode on the battery performance is discussed.

4. Conclusions

In conclusion, the results of this study revealed that the addition of LiTFSI to the cathodes of SSLBs can significantly affect their electrochemical properties. FESEM analysis revealed that the addition of LiTFSI reduced delamination between the positive electrode sheet and the electrolyte membrane. In addition, the EIS results revealed that the LiTFSI-based cathode exhibited a smaller total resistance value, indicating lower hindrance in the internal lithium-ion transport path and smaller interface resistance. Additionally, the discharge capacity of the battery assembled using the cathode containing 3% LiTFSI was 168.9 mAhg^{-1} at 0.1 C, which is close to the theoretical capacity (170 mAhg^{-1}), and the battery demonstrated stability during high-rate charging and discharging. When charging at a high rate of 0.5 C, the discharge capacity of the battery reached 161.8 mAhg^{-1} , with a capacity retention rate as high as 94%, when charging at a high rate and switching back to low-rate charging (0.1 C), indicating that the battery maintained strong stability even after high-rate charging and discharging. In summary, this result indicates that the addition of an appropriate amount of LiTFSI can effectively enhance the electrochemical performance of the battery, with the optimal performance achieved at an LiTFSI ratio of 3%. Future studies will focus on improving the synthesis of LiFePO_4 -lithium salt composite cathodes to achieve a more uniform and stable composite structure; optimize the composition of

the composite material; and enhance understanding of the electrochemical behavior of the composite cathode.

Author Contributions: D.M., conceptualization, methodology, investigation, data curation, writing—original draft preparation; P.-H.H., investigation, data curation, formal analysis; I.-M.H., conceptualization, supervision, funding acquisition, writing—review and editing. All authors have read and agreed to the published version of the manuscript.

Funding: Financial support for this work was provided by the National Science and Technology Council in Taiwan through grant numbers: NSTC 111-2622-E-155-011 and MOST 110-2623-E-155-011.

Data Availability Statement: The data that support the findings of this study are available from the corresponding author upon reasonable request.

Conflicts of Interest: The authors declare no conflict of interest.

References

1. Chen, T.; Jin, Y.; Lv, H.; Yang, A.; Liu, M.; Chen, B.; Xie, Y.; Chen, Q. Applications of Lithium-Ion Batteries in Grid-Scale Energy Storage Systems. *Trans. Tianjin Univ.* **2020**, *26*, 208–217. [[CrossRef](#)]
2. Santamaria, C.; Morales, E.; Rio, C.D.; Herradon, B.; Amarilla, J.M. Studies on sodium-ion batteries: Searching for the proper combination of the cathode material, the electrolyte and the working voltage. The role of magnesium substitution in layered manganese-rich oxides, and pyrrolidinium ionic liquid. *Electrochim. Acta* **2023**, *439*, 141654–141663. [[CrossRef](#)]
3. Wang, H.; Chen, S.; Li, Y.; Liu, Y.; Jing, Q.; Liu, X.; Liu, Z.; Zhang, X. Organosilicon-Based Functional Electrolytes for High-Performance Lithium Batteries. *Adv. Energy Mater.* **2021**, *11*, 2101057–2101082. [[CrossRef](#)]
4. Gür, T.M. Review of electrical energy storage technologies, materials and systems: Challenges and prospects for large-scale grid storage. *Energy Environ. Sci.* **2018**, *11*, 2696–2767. [[CrossRef](#)]
5. Liu, Y.; Zhang, R.; Wang, J.; Wang, Y. Current and future lithium-ion battery manufacturing. *iScience* **2021**, *24*, 102332–102348. [[CrossRef](#)] [[PubMed](#)]
6. Zheng, J.; Kim, M.S.; Tu, Z.; Choudhury, S.; Tang, T.; Archer, L.A. Regulating electrodeposition morphology of lithium: Towards commercially relevant secondary Li metal batteries. *Chem. Soc. Rev.* **2020**, *49*, 2701–2750. [[CrossRef](#)]
7. Li, Y.; Wang, L.; Zhang, K.; Liang, F.; Yao, Y.; Kong, L. High performance of LiFePO₄ with nitrogen and phosphorus dual-doped carbon layer for lithium-ion batteries. *J. Alloys Compd.* **2022**, *890*, 161617–161624. [[CrossRef](#)]
8. Nirmale, T.C.; Karbhal, I.; Kalubarme, R.S.; Shelke, M.V.; Varma, A.J.; Kale, B.B. Facile Synthesis of Unique Cellulose Triacetate Based Flexible and High Performance Gel Polymer Electrolyte for Lithium Ion Batteries. *ACS Appl. Mater. Interfaces* **2017**, *9*, 34773–34782. [[CrossRef](#)]
9. He, P.; Yu, H.; Li, D.; Zhou, H. Layered lithium transition metal oxide cathodes towards high energy lithium-ion batteries. *J. Mater. Chem.* **2012**, *22*, 3680–3695. [[CrossRef](#)]
10. Vicente, N.; Haro, M.; Cintora-Juarez, D.; Perez-Vicente, C.; Tirado, J.L.; Ahmad, S.; Garcia-Belmonte, G. LiFePO₄ particle conductive composite strategies for improving cathode rate capability. *Electrochim. Acta* **2015**, *163*, 323–329. [[CrossRef](#)]
11. Ramasubramanian, B.; Sundarrajan, S.; Chellappan, V.; Reddy, M.V.; Ramakrishna, S.; Zaghbi, K. Recent Development in Carbon-LiFePO₄ Cathodes for Lithium-Ion Batteries: A Mini Review. *Batteries* **2022**, *8*, 133. [[CrossRef](#)]
12. Lei, W.; Li, H.; Tang, Y.; Shao, H. Progress and perspectives on electrospinning techniques for solid-state lithium batteries. *Carbon Energy* **2022**, *4*, 539–575. [[CrossRef](#)]
13. Wang, K.; Chen, Y.; Zhang, L.; Zhang, Q.; Cheng, Z.; Su, Y.; Shen, F.; Han, X. One step hot-pressing method for hybrid Li metal anode of solid-state lithium metal batteries. *J. Mater. Sci. Technol.* **2023**, *153*, 32–40. [[CrossRef](#)]
14. Heng, S.; Shi, Q.; Zheng, X.; Wang, Y.; Qu, Q.; Liu, G.; Battaglia, V.S.; Zheng, H. An organic-skinned secondary coating for carbon-coated LiFePO₄ cathode of high electrochemical performances. *Electrochim. Acta* **2017**, *258*, 1244–1253. [[CrossRef](#)]
15. Kim, D.H.; Kim, J. Synthesis of LiFePO₄ Nanoparticles in Polyol Medium and Their Electrochemical Properties. *Electrochem. Solid-State Lett.* **2006**, *9*, A439–A442. [[CrossRef](#)]
16. Moreno, M.G.; Fernandez, G.M.; Mysyk, R.; Carriazo, D. A high-energy hybrid lithium-ion capacitor enabled by a mixed capacitive-battery storage LiFePO₄—AC cathode and a SnP₂O₇—rGO anode. *Sustain. Energy Fuels* **2023**, *7*, 965–976. [[CrossRef](#)]
17. Rosaiah, P.; Kumar, P.J.; Babu, K.J.; Hussain, O.M. Electrical and electrochemical properties of nanocrystalline LiFePO₄ cathode. *Appl. Phys. A* **2013**, *113*, 603–611. [[CrossRef](#)]
18. Liu, X.; Sun, L.; Vu, N.H.; Linh, D.T.H.; Dien, P.T.; Hoa, L.T.; Lien, D.T.; Nang, H.X.; Dao, V.D. Synthesis of LiFePO₄/carbon/graphene for high-performance Li-ion battery. *J. Electroanal. Chem.* **2023**, *932*, 117205–117210. [[CrossRef](#)]
19. Wu, H.; Liu, Q.; Guo, S. Composites of Graphene and LiFePO₄ as Cathode Materials for Lithium-Ion Battery: A Mini-review. *Nano-Micro Lett.* **2014**, *6*, 316–326. [[CrossRef](#)]
20. Balo, L.; Gupta, H.; Singh, S.K.; Singh, V.K.; Tripathi, A.K.; Srivastava, N.; Tiwari, R.K.; Mishra, R.; Meghnani, D.; Singh, R.K. Development of gel polymer electrolyte based on LiTFSI and EMIMFSI for application in rechargeable lithium metal battery with GO-LFP and NCA cathodes. *J. Solid State Electrochem.* **2019**, *23*, 2507–2518. [[CrossRef](#)]

21. Wei, X.; Guan, Y.; Zheng, X.; Zhu, Q.; Shen, J.; Qiao, N.; Zhou, S.; Xu, B. Improvement on high rate performance of LiFePO₄ cathodes using graphene as a conductive agent. *Appl. Surf. Sci.* **2018**, *440*, 748–754. [[CrossRef](#)]
22. Falco, M.; Simari, C.; Ferrara, C.; Nair, J.R.; Meligrana, G.; Bella, F.; Nicotera, I.; Mustarelli, P.; Winter, M.; Gerbaldi, C. Understanding the Effect of UV-Induced Cross-Linking on the Physicochemical Properties of Highly Performing PEO/LiTFSI-Based Polymer Electrolytes. *Langmuir* **2019**, *35*, 8210–8219. [[CrossRef](#)] [[PubMed](#)]
23. Karuppasamy, K.; Antony, R.; Alwin, S.; Balakumar, S.; Shajan, X.S. A Review on PEO Based Solid Polymer Electrolytes (SPEs) Complexed with LiX (X=Tf, BOB) for Rechargeable Lithium Ion Batteries. *Mater. Sci. Forum* **2015**, *807*, 41–63. [[CrossRef](#)]
24. Chen, L.; Qiu, X.; Bai, Z.; Fan, L.Z. Enhancing interfacial stability in solid-state lithium batteries with polymer/garnet solid electrolyte and composite cathode framework. *J. Energy Chem.* **2021**, *52*, 210–217. [[CrossRef](#)]
25. Chen, H.; Adekoya, D.; Hencz, L.; Ma, J.; Chen, S.; Yan, C.; Zhao, H.; Cui, G.; Zhang, S. Stable Seamless Interfaces and Rapid Ionic Conductivity of Ca–CeO₂/LiTFSI/PEO Composite Electrolyte for High-Rate and High-Voltage All-Solid-State Battery. *Adv. Energy Mater.* **2020**, *10*, 2000049–2000061. [[CrossRef](#)]
26. Chen, X.; He, W.; Ding, L.X.; Wang, S.; Wang, h. Enhancing interfacial contact in all solid state batteries with a cathode-supported solid electrolyte membrane framework. *Energy Environ. Sci.* **2019**, *12*, 938–944. [[CrossRef](#)]
27. Li, Z.; Liu, Y.; Liang, X.; Yu, M.; Liu, B.; Sun, Z.; Hu, W.; Zhu, G. A single-ion gel polymer electrolyte based on polyimide grafted with lithium 3-chloropropanesulfonyl (trifluoromethanesulfonyl) imide for high performance lithium ion batteries. *J. Mater. Chem. A* **2023**, *11*, 1766–1773. [[CrossRef](#)]
28. Stenina, I.; Pyrkova, A.; Yaroslavtsev, A. NASICON-Type Li_{1+x}Al_xZr_yTi_{2-x-y}(PO₄)₃ Solid Electrolytes: Effect of Al, Zr Co-Doping and Synthesis Method. *Batteries* **2023**, *9*, 59. [[CrossRef](#)]
29. Zhang, Q.K.; Zhang, X.Q.; Yuan, H.; Huang, J.Q. Thermally Stable and Nonflammable Electrolytes for Lithium Metal Batteries: Progress and Perspectives. *Small Sci.* **2021**, *1*, 2100058–2100071. [[CrossRef](#)]
30. Li, W.; Chen, L.; Sun, Y.; Wang, C.; Wang, Y.; Xia, Y. All-solid-state secondary lithium battery using solid polymer electrolyte and anthraquinone cathode. *Solid State Ion.* **2017**, *300*, 114–119. [[CrossRef](#)]
31. Cheng, D.; Sun, C.; Lang, Z.; Zhang, J.; Hu, A.; Duan, J.; Chen, X.; Zang, H.Y.; Chen, J.; Zheng, M.; et al. Hybrid covalent organic-framework-based electrolytes for optimizing interface resistance in solid-state lithium-ion batteries. *Cell Rep. Phys. Sci.* **2022**, *3*, 100731–100743. [[CrossRef](#)]
32. Li, C.; Wang, Z.Y.; He, Z.J.; Li, Y.J.; Mao, J.; Dai, K.H.; Yan, C.; Zheng, J.C. An advance review of solid-state battery: Challenges, progress and prospects. *Sustain. Mater. Technol.* **2021**, *29*, e00297–e00310. [[CrossRef](#)]
33. Shen, S.P.; Tang, G.; Li, H.J.; Zhang, L.; Zheng, J.C.; Luo, Y.; Yue, J.P.; Shi, Y.; Chen, Z. Low-temperature fabrication of NASICON-type LATP with superior ionic conductivity. *Ceram. Int.* **2022**, *48*, 36961–36967. [[CrossRef](#)]
34. Pogosova, M.A.; Krasnikova, I.V.; Sanin, A.O.; Lipovskikh, S.A.; Eliseev, A.A.; Sergeev, A.V.; Stevenson, K.J. Complex Investigation of Water Impact on Li-Ion Conductivity of Li_{1.3}Al_{0.3}Ti_{1.7}(PO₄)₃—Electrochemical, Chemical, Structural, and Morphological Aspects. *Chem. Mater.* **2020**, *32*, 3723–3732. [[CrossRef](#)]
35. Xue, X.; Zhang, X.; Liu, Y.; Chen, S.; Chen, Y.; Lin, J.; Zhang, Y. Boosting the Performance of Solid-State Lithium Battery Based on Hybridizing Micron-Sized LATP in a PEO/PVDF-HFP Heterogeneous Polymer Matrix. *Energy Technol.* **2020**, *8*, 2000444–2000468. [[CrossRef](#)]
36. Yao, Z.; Zhu, K.; Li, X.; Zhang, J.; Li, J.; Wang, J.; Yan, K.; Liu, J. Double-Layered Multifunctional Composite Electrolytes for High-Voltage Solid-State Lithium-Metal Batteries. *ACS Appl. Mater. Interfaces* **2021**, *13*, 11958–11967. [[CrossRef](#)] [[PubMed](#)]
37. Janek, J.; Zeier, W.G. A solid future for battery development. *Nat. Energy* **2016**, *1*, 16141–16144. [[CrossRef](#)]
38. Shi, X.; Ma, N.; Wu, Y.; Lu, Y.; Xiao, Q.; Li, Z.; Lei, G. Fabrication and electrochemical properties of LATP/PVDF composite electrolytes for rechargeable lithium-ion battery. *Solid State Ion.* **2018**, *325*, 112–119. [[CrossRef](#)]
39. Zhang, Q.; Wang, Q.; Huang, S.; Jiang, Y.; Chen, Z. Preparation and electrochemical study of PVDF-HFP/LATP/g-C₃N₄ composite polymer electrolyte membrane. *Inorg. Chem. Commun.* **2021**, *131*, 108793–108799. [[CrossRef](#)]
40. Mohanty, D.; Lu, Z.L.; Hung, I.M. Effect of carbon coating on electrochemical properties of Li₃V₂(PO₄)₃ cathode synthesized by citric-acid gel method for lithium-ion batteries. *J. Appl. Electrochem.* **2022**, *52*, 1003–1013. [[CrossRef](#)]
41. Mohanty, D.; Chen, S.Y.; Hung, I.M. Effect of Lithium Salt Concentration on Materials Characteristics and Electrochemical Performance of Hybrid Inorganic/Polymer Solid Electrolyte for Solid-State Lithium-Ion Batteries. *Batteries* **2022**, *8*, 173. [[CrossRef](#)]
42. Hsieh, C.T.; Pai, C.T.; Chen, Y.F.; Chen, I.L.; Chen, W.Y. Preparation of lithium iron phosphate cathode materials with different carbon contents using glucose additive for Li-ion batteries. *J. Taiwan Inst. Chem. Eng.* **2014**, *45*, 1501–1508. [[CrossRef](#)]
43. Nien, Y.H.; Carey, J.R.; Chen, J.S. Physical and electrochemical properties of LiFePO₄/C composite cathode prepared from various polymer-containing precursors. *J. Power Source* **2009**, *193*, 822–827. [[CrossRef](#)]
44. Wu, H.C.; Wu, H.C.; Lee, E.; Wu, N.L. High-temperature carbon-coated aluminum current collector for enhanced power performance of LiFePO₄ electrode of Li-ion batteries. *Electrochem. Commun.* **2010**, *12*, 488–491. [[CrossRef](#)]
45. Jaumaux, P.; Liu, Q.; Zhou, D.; Xu, X.; Wang, Y.; Kang, F.; Li, B.; Wang, G. Deep-Eutectic-Solvent-Based Self-Healing Polymer Electrolyte for Safe and Long-Life Lithium-Metal Batteries. *Angew. Chem. Int. Ed.* **2020**, *59*, 9134–9142. [[CrossRef](#)]
46. Nilsson, V.; Bernin, D.; Brandell, D.; Edstrom, K.; Johansson, P. Interactions and Transport in Highly Concentrated LiTFSI-based Electrolytes. *ChemphysChem* **2020**, *21*, 1166–1176. [[CrossRef](#)]

47. Atik, J.; Diddens, D.; Thienenkamp, J.H.; Brunklaus, G.; Winter, M.; Pillard, E. Cation-Assisted Lithium-Ion Transport for High-Performance PEO-based Ternary Solid Polymer Electrolytes. *Angew. Chem. Int. Ed.* **2021**, *60*, 11919–11927. [[CrossRef](#)]
48. Chen, S.Y.; Hsieh, C.T.; Zhang, R.S.; Mohanty, D.; Gandomi, Y.A.; Hung, I.M. Hybrid solid state electrolytes blending NASICON-type $\text{Li}_{1+x}\text{Al}_x\text{Ti}_{2-x}(\text{PO}_4)_3$ with poly(vinylidene fluoride-co-hexafluoropropene) for lithium metal batteries. *Electrochim. Acta* **2022**, *427*, 140903. [[CrossRef](#)]

Disclaimer/Publisher's Note: The statements, opinions and data contained in all publications are solely those of the individual author(s) and contributor(s) and not of MDPI and/or the editor(s). MDPI and/or the editor(s) disclaim responsibility for any injury to people or property resulting from any ideas, methods, instructions or products referred to in the content.